Spatial and Temporal Variation in Slip Rate along the Kongur Normal Fault, Chinese Pamir

Lindsay M Schoenbohm[1], Ji Chen[2], Zhaode Yuan[2], Benjamin Kirby[3], Edward R Sobel[4], Lewis A Owen[5]

[1] Department of Chemical and Physical Sciences, University of Toronto Mississauga, Mississauga, ON L5L 1C6, Canada, lindsay.schoenbohm@utoronto.ca
[2] State Key Lab. of Earthquake Dynamics, Inst. of Geology, China Earthquake Admin., PO Box 9803, Beijing, 100029, China
[3] Anadarko Petroleum Corp., Houston, TX, 77380, USA
[4] Institute für Erd- und Umweltwissenschaften, Universität Potsdam, 14476 Potsdam, Germany
[5] Department of Geology, University of Cincinnati, Cincinnati, OH 45221, USA

Much of the interior of the Pamir Mountains experience approximately E-W extension, despite their location within the convergent western Himalayan syntaxis. Extension could reflect radial overthrusting or oroclinal bending of the Pamir, or reflect differential shortening, but the precise driver remains poorly understood. The Kongur normal fault (Fig. 1) in the Chinese Pamir has been extending since ~7-8 Ma in the north and 7-5.5 Ma in the south (Robinson et al., 2004; 2007). The Muji segment of the fault in the north strikes E-W and is dominated by right-lateral strike-slip displacement. To the south, the fault strikes NW-SE or N-S, forming excursions around the anomalously high peaks Kongur Shan (7,719 m) and Muztagh Ata (7,546 m), which sit the in footwall of the fault. These peaks are underlain by deeply exhumed rocks. Exhumation dies off rapidly to the south and is transferred via the NW-dipping Tahaman fault to the E-dipping Tashkorgan fault. The correspondence between the high peaks and large glaciers and an inferred 8-fold acceleration in exhumation rate at ~ 2 Ma (Arnaud et al., 1993), has led to the suggestion that enhanced exhumation is a response to glacial erosion in the Quaternary. However, while glacier morphology does seem to reflect exhumation rate, lithology and erosion along the Gez River appear more closely linked with the degree of unroofing and formation of the high peaks than does glacial erosion (Schoenbohm et al., in review). Additionally, thermochronologic modelling (Robinson et al., 2004; 2010) suggest constant cooling since ~7-8 Ma. To better understand the nature of extension in the Pamir and to test models for climate-tectonic coupling in the footwall of the fault, both short- and long-tem slip rate along the Kongur normal fault need to be defined.

Exhumation along a dipping fault and advection of isotherms makes determination of long term displacement rate from cooling data problematic. Thermo-kinematic modelling has only been completed along a transect through the footwall where the Gez River crosses the range; the study demonstrates that slip along the fault has been steady at ~6.5 mm/yr since 7 Ma (Robinson et al., 2010). Assuming a 40° west-dipping fault this indicates a vertical displacement rate of 4.2 mm/yr (Fig. 2) an E-W extension rate of 5.0 mm/yr and (Fig. 1), nearly identical to the GPS-determined rate of 5.1 ± 0.8 mm/yr (Yang et al., 2008; Zubovich et al., 2010). ^{40}Ar/^{39}Ar biotite and muscovite, and zircon (U-Th)/He data show a similar pattern, with the youngest ages near the center of the fault (Fig. 2). These data suggest a consistent pattern of maximum vertical and horizontal displacement rates in the center of the Kongur detachment.

To define short-term rates, offset fluvial terraces and moraines were mapped and dated using ^{10}Be terrestrial cosmogenic nuclides (TCN). Mapping was conducted using real time kinematic GPS. Terraces were dated by collecting a series of samples from 2-m deep pits along the terrace edges and analyzing the samples for ^{10}Be TCN concentration. For moraine dating, 5 samples were collected from the surface of large, partially-embedded boulders. Samples were processed following standard methods and analyzed at the PRIME Lab facility. We modelled TCN concentration using a Monte Carlo method developed by Hidy et al. (2010). Along the dominantly strike-slip Muji segment of the fault, we dated two terraces ($9.9^{+1.8}_{-1.2}$ ka and $3.3^{+0.6}_{-0.6}$ ka) and two moraines (30.8 ± 5.8 ka and 12.3 ± 2.7 ka). The inner riser between the lower and upper terrace, which is offset 37.6 m, has been preserved at least since the abandonment of the lower terrace, and therefore indicates a dextral slip rate of 11.4 mm/yr ± 2.1. The younger moraine is offset 169 m across the fault, indicating dextral slip at 13.7 mm/yr ± 3.0, the same within uncertainty, suggesting an average rate of ~12.6 mm/yr (Fig. 1). This is slightly faster than the 8.1 ± 0.9 mm/yr suggested by GPS data (Yang et al., 2008; Zubovich et al., 2010). Along the northern section of the dip-slip part of the Kongur detachment fault, a terrace offset 20 m vertically was dated at $6.6^{+1.0}_{-1.0}$ ka. This suggests a vertical offset rate of 3.0 ± 0.5 mm/yr and an E-W extension rate (assuming a 20° west-dipping fault because of the oblique extension direction) of 8.3 ± 1.4 mm/yr. This rate is similar to but still slightly higher than the GPS derived rate of 7.5 ± 0.8 mm/yr (Yang et al., 2008; Zubovich et al., 2010). Additional antithetic faults within the hanging wall valley accommodate further extension, and could make up the difference in horizontal extension between the two sites.

Holocene slip rate along the Kongur normal fault is similar to the modern GPS rates, but considerably faster than the long-term slip rate as indicated by thermochronologic data. One explanation may be that the study captures a particularly active period of the earthquake cycle, and our rates are thus not representative. However, an intriguing possibility is that slip rate has recently increased, implying accelerated E-W extension. It is unclear however, what could have driven such acceleration. Further, extension rates are faster in the north, despite the greater exhumation of the central part of the fault.

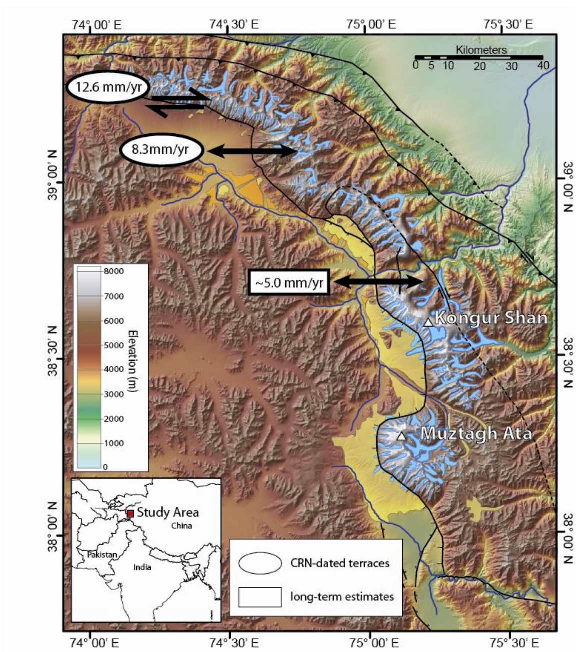

Figure 1. Map (SRTM DEM base) of study region showing E-W horizontal extension along the Kongur normal fault.

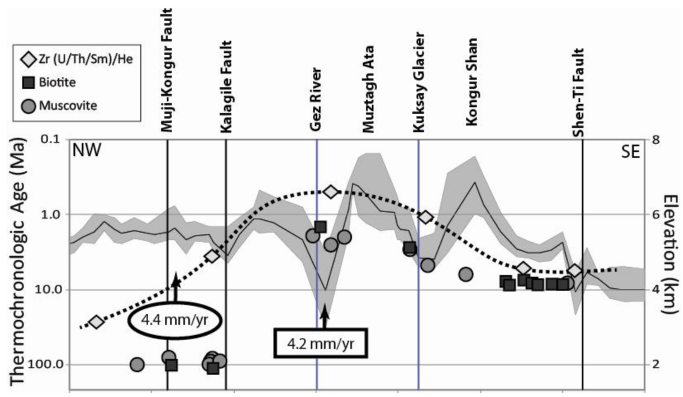

Figure 2. Data from NW to SE along Kongur normal fault. Thermochronologic data from Robinson et al., 2004; 2007 and Schoenbohm et al., in review. Dashed line connects zircon (U-Th)/He data in order to schematically depict maximum cooling rate near center of fault system. grey region with center line shows max, min and mean topography. Symbols for vertical exhumation rate same as for Figure 1.

References

Arnaud, N.O., M. Brunel, J.M. Cantagrel, and P. Tapponnier (1993), High cooling and denudation rates at Kongur Shan, eastern Pamir (Xinjiang, China) revealed by $^{40}Ar/^{39}Ar$ alkali feldspar thermochronology, *Tectonics*, *12*, 1335-1346.

Hidy, A.J., J.C. Gosse, J.L. Pederson, J.P. Mattern and R.C. Finkel (2010), A geologically constrained Monte Carlo approach to modeling exposure ages from profiles of cosmogenic nuclides: an example from Lees Ferry, AZ: *Geochemistry, Geophysics and Geosystems*, v. 11, doi: 10.1029/2010GC003084.

Robinson, A.C., A. Yin, C.E. Manning, T.M. Harrison, Zhang S., Wang X (2004), Tectonic evolution of the northeastern Pamir: Constraints from the northern portion of the Cenozoic Kongur Shan extensional system, western China, *Geological Society of America Bulletin*, *116*, 953-973.

Robinson, A.C., A. Yin, C.E. Manning, T.M. Harrison, Zhang S. and Wang X. (2007), Cenozoic evolution of the eastern Pamir: Implications for strain-accommodation mechanisms at the western end of the Himalayan-Tibetan orogen, *Geological Society of America Bulletin*, *119*, 882-896.

Robinson, A.C., A. Yin, and O.M. Lovera (in press), The role of footwall deformation and denudation in controlling cooling age patterns of detachment systems: An application to the Kongur Shan extensional system in the Eastern Pamir, China, *Tectonophysics*, doi: 10.1016/j.tecto.1020.10.003.

Sobel, E.R., Schoenbohm, L., Chen, J., Thiede, R., Stockli, D., Sudo, M., and Strecker, M.R., 2011, Late Miocene - Pliocene deceleration of dextral slip between Pamir and Tarim: Implications for Pamir orogenesis: Earth and Planetary Science Letters, v. 304, p. 369-378.

Yang S, Li J, Wang Q., 2008, The deformation pattern and fault rate in the Tianshan Mountains inferred from GPS observation: Science in China Series D: Earth Science, v. 51, p. 1064-1080.

Zubovich A V, Wang X Q, Scherba Y G *et al*., 2010, GPS velocity field of the Tien Shan and surrouding region: Tectonics, v. 29, doi: 10.1029/2010TC002772.